Fungal Genetics and Biology 90 (2016) 12–22

Contents lists available at ScienceDirect

Fungal Genetics and Biology

journal homepage: www.elsevier.com/locate/yfgbi

Chasing stress signals – Exposure to extracellular stimuli differentially affects the redox state of cell compartments in the wild type and signaling mutants of *Botrytis cinerea*

Robert Marschall, Julia Schumacher, Ulrike Siegmund, Paul Tudzynski *

Institut für Biologie und Biotechnologie der Pflanzen, Westfälische Wilhelms-Universität, Schlossplatz 8, D-48143 Münster, Germany

ARTICLE INFO

Article history:
Received 19 January 2016
Revised 26 February 2016
Accepted 13 March 2016
Available online 14 March 2016

Keywords:
Phytopathogenic fungi
Redox signaling
Botrytis cinerea
roGFP2
Stress

ABSTRACT

Reactive oxygen species (ROS) are important molecules influencing intracellular developmental processes as well as plant pathogen interactions. They are produced at the infection site and affect the intracellular redox homeostasis. However, knowledge of ROS signaling pathways, their connection to other signaling cascades, and tools for the visualization of intra- and extracellular ROS levels and their impact on the redox state are scarce. By using the genetically encoded biosensor roGFP2 we studied for the first time the differences between the redox states of the cytosol, the intermembrane space of mitochondria and the ER in the filamentous fungus *Botrytis cinerea*. We showed that the ratio of oxidized to reduced glutathione inside of the cellular compartments differ and that the addition of hydrogen peroxide (H_2O_2), calcium chloride ($CaCl_2$) and the fluorescent dye calcofluor white (CFW) have a direct impact on the cellular redox states. Dependent on the type of stress agents applied, the redox states were affected in the different cellular compartments in a temporally shifted manner. By integrating the biosensor in deletion mutants of *bcnoxA*, *bcnoxB*, *bctrx1* and *bcltf1* we further elucidated the putative roles of the different proteins in distinct stress-response pathways. We showed that the redox states of Δ*bcnoxA* and Δ*bcnoxB* display a wild-type pattern upon exposure to H_2O_2, but appear to be strongly affected by $CaCl_2$ and CFW. Moreover, we demonstrated the involvement of the light-responsive transcription factor BcLtf1 in the maintenance of the redox state in the intermembrane space of the mitochondria. Finally, we report that $CaCl_2$ as well as cell wall stress-inducing agents stimulate ROS production and that Δ*bcnoxB* produces significantly less ROS than the wild type and Δ*bcnoxA*.

1. Introduction

One of the most destructive plant pathogens is the filamentous fungus *Botrytis cinerea* (Dean et al., 2012). The pathogen is infecting more than 500, in most cases dicotyledonous plant species (Elad et al., 2016). Under favorable conditions the conidiospores attach to the host, penetrate the surface and finally colonize the plant tissues. The infection process is facilitated by the secretion of cell wall-degrading enzymes (ten Have et al., 1998) and phytotoxic compounds (Dalmais et al., 2011) as well as by the production of reactive oxygen species (ROS) (Govrin and Levine, 2000; Marschall and Tudzynski, 2014). The fungus is also able to survive unfavorable conditions, such as low temperatures, by resting in a quiescent growth phase (Elad et al., 2007). Within plant-pathogen interactions, plants react to pathogen-derived elicitors by producing ROS during the so called 'oxidative burst' as one of their first defence mechanisms (Levine et al., 1994). ROS (H_2O_2, O_2^-, ·HO) additionally play an important role in various differentiation and developmental processes, such as polarized growth and the formation of fungal infection structures (Scott and Eaton, 2008); they have a diffusible nature and serve as signaling molecules in small amounts. However, in higher concentrations they are harmful because they interact non-specifically with macromolecules such as DNA, proteins and lipids (Beckman and Ames, 1998). Within the equilibrium of non-stimulated cells ROS are produced in highly conserved processes. On one hand, they arise as mere by-products of the respiratory chain; on the other hand they occur as a result of evolved enzymatic reactions within signaling cascades or during defence reactions.

NADPH oxidase (Nox) complexes are one of the major sources of enzymatically produced ROS: they transfer electrons across membranes from NADPH to molecular oxygen (Tudzynski et al., 2012). Nox are best understood in the mammalian system where localization, functions and mechanisms are widely elucidated. Although many aspects of their function in fungi are still unknown, there is increasing evidence of structural/functional homologies between Nox complexes in mammals and fungi, despite of the

* Corresponding author.
E-mail address: tudzyns@uni-muenster.de (P. Tudzynski).

http://dx.doi.org/10.1016/j.fgb.2016.03.002
1087-1845/

evolutionary distance. For example, homologs of the regulatory subunit (p67phox/NoxR), the catalytic subunit (gp91phox/Nox1/2 or NoxA/B) as well as other regulatory compounds (p22phox/NoxD) (Cano-Dominguez et al., 2008; Egan et al., 2007; Lacaze et al., 2015; Lara-Ortiz et al., 2003; Malagnac et al., 2004; Segmueller et al., 2008; Semighini and Harris, 2008; Siegmund et al., 2013, 2015) have been already identified and characterized. To handle elevated levels of ROS, eukaryotic cells have evolved scavenging systems to establish and maintain an equilibrium. An enzymatic degradation of ROS is accomplished by the superoxide dismutase (SOD) which converts superoxide (O_2^-) into hydrogen peroxide (H_2O_2) as well as by peroxidases and catalases that catalyze the further degradation of H_2O_2. The non-enzymatic detoxification is conducted by the reaction with small soluble molecules such as carotenoids, flavonoids, ascorbic acid and glutathione. Reduced glutathione (GSH) is regenerated to its oxidized form (GSSG) by the glutathione reductase that uses NADPH as an electron donor (Apel and Hirt, 2004). The glutathione pool (ratio of GSH/GSSG) therefore reflects the redox state of the cell. To avoid loss of redox homeostasis, cells try to maintain a high ratio of GSH to GSSG (Hwang et al., 1992; Appenzeller-Herzog, 2011). Besides the glutathione system, thioredoxins – highly conserved oxidoreductases – contribute to the intracellular redox balance by facilitating the reduction of target proteins by thiol-disulfide exchange reactions. They are regenerated by the thioredoxin reductase and thus prevent as antioxidative system the unfolded protein response (UPR) by thiol exchange reactions (Arner and Holmgren, 2000; Trotter and Grant, 2002). Additionally, thioredoxins affect processes such as dNTP generation (Koc et al., 2006) or the reduction of methionine sulfoxide and sulfate (Gonzalez Porque et al., 1970). In *B. cinerea* it was already shown that the losses of the cytosolic thioredoxin (BcTrx1) and the thioredoxin reductase (BcTrr1) affect pathogenicity as well as the adequate response to oxidative stress. However, no indications were found that BcTrx1 influences the cytosolic glutathione pool (Viefhues et al., 2014).

Apart from enzymes that are either directly involved in the production of ROS, such as the Nox complex, or might contribute as antioxidants to the redox homeostasis, such as BcTrx1, there are several other proteins that affect the dynamic balance of ROS production and scavenging. Hence, the light-responsive transcription factor BcLtf1 plays an essential role in maintaining the ROS homeostasis and mediating the tolerance to exogenous oxidative stress; moreover, it modulates the light responses and the production of secondary metabolites (melanin, botrydial and botcinic acid) in *B. cinerea* (Schumacher et al., 2014).

In this study, we describe the redox state of different cellular compartments of *B. cinerea*, i.e. in the cytosol, the intermembrane space of the mitochondria and the endoplasmic reticulum (ER) and how the redox state changed in response to the exposure to the oxidant H_2O_2, to $CaCl_2$ and cell wall stress-inducing agents. For this purpose, we used modified versions of a redox-sensitive reporter (roGFP2) that are targeted to above mentioned cellular compartments. Besides the wild-type strain, we studied the redox states in knock-out mutants of proteins which have been assumed to affect the maintenance of the redox state, such as members of the Nox complexes (NoxA/B), the thioredoxin system (Trx1), as well as the light-responsive transcription factor 1 (Ltf1).

2. Materials and methods

2.1. Cultivation of B. cinerea

B. cinerea Pers.:Fr. [*Botryotinia fuckeliana* (de Bary)Whetzel] B05.10 was isolated from *Vitis vinifera* (Buettner et al., 1994) and was used in this study for the integration of the redox sensor and as wild-type control in all experiments. Additional strains are listed in Table S2.

Strains were grown on synthetic complete medium (CM) (Pontecorvo et al., 1953). For transformation, the strains were grown on PDAB medium (Potato dextrose agar [Sigma–Aldrich Chemie, Steinheim, Germany] supplemented with 100 g/l homogenized leaves of French beans (*Phaeseolus vulgaris*). For the production of conidia, strains were incubated for 6–8 days at 20 °C under light conditions (12 h light/12 h darkness, full spectrum light); to obtain sclerotia, strains were grown 3 weeks at 20 °C in darkness. For the preparation of DNA, the strains were grown 3–4 days at 18 °C on CM agar with Cellophane overlays.

2.2. Generation of mutants expressing roGFP2 in the cytosol, the mitochondria or the ER

To generate reporter gene constructs for targeting roGFP2 to different cellular compartments, the homologous recombination system in yeast was applied (Schumacher, 2012). For the cytosolic expression of the redox sensor, the construct generated previously (Heller et al., 2012a, 2012b) was used (selection via hygromycin). In addition, a construct for selection via nourseothricin was generated by amplifying the reporter gene with the primers 1/2 (Fig. S1/Table S3). The construct was integrated into the appropriate expression vectors (Schumacher, 2012) under the control of the constitutive *oli*C promoter of *Aspergillus nidulans*. The respective plasmids were digested with *Nco*I/*Not*I; the amplified reporter gene fragment contained overlaps to P*oli*C as well as to the glucanase terminator (T*gluc*). Homologous recombination took place in the *S. cerevisiae* strain FY834. Positive transformants were selected on SD-plates lacking uracil and the total DNA was isolated and transformed in *Escherichia coli*. The plasmids from *S. cerevisiae* and *E. coli* were isolated by the Nucleo spin® plasmid easypure kit (Macherey-Nagel, Düren, Germany) and correct assembly was tested by sequencing.

For targeting the redox sensor to the ER, the HDEL motif was added to the 3′-end of the reporter gene by the primers 10/12 or 10/13 as well as 1/11 (Table S3). To target roGFP2 to the mitochondrial intermembrane space, the first 31 aa of cytochrome C were cloned (primers 4/5) to the 5′-end of the reporter gene and fused into the appropriate expression vector by use of the primers 2/3 (Fig. S1/Table S3). Afterwards the constructs were processed as described above. For transformation of *B. cinerea* the expression cassettes were excised by digestion with *Apa*I/*Sac*II.

Transformation of *B. cinerea* was performed as described previously (Gronover et al., 2001). Transformants were selected by hygromycin (70 μg/ml of hygromycin B [Invitrogen, San Diego, USA] or nourseothricin (50 μg/ml of nourseothricin [Werner-Bioagents, Jena, Germany] resistance. The purification was done by single spore isolation. For this, conidia were spread on the respective selective medium. Germinated conidia were picked and cultivated. The correct integrations of the constructs were proved with primer combinations 6–9 or 14–17 via diagnostic PCR. For this purpose, genomic DNA was isolated according to Cenis (Cenis, 1992).

2.3. Growth and pathogenicity assays

To establish that the integration of the biosensor has no influence on the phenotype of the respective mutants, different growth and pathogenicity assays were performed. Nutrient-dependent germination on glass surfaces was monitored according to Doehlemann et al. (2006), while the pathogenicity was confirmed on French bean plants (*P. vulgaris* L.) with agar plugs of fresh mycelium or conidia from freshly sporulated PDAB-agar plates, as described by Klimpel et al. (2002). The penetration of the bean epidermis was checked as described previously (Siegmund et al., 2015).

2.4. Quantification of ROS accumulation

The detection of ROS was performed using the Enzo Life Science Total ROS/Superoxide Detection Kit (Enzo Life Science, Lausen, Switzerland), comprising two detection agents that detect superoxide or ROS simultaneously and specifically. The detection mix was prepared as described in the instruction manual. For visualization of ROS during different differentiation processes, the detection mix was added just before microscopy in the ratio 1:10 (Marschall and Tudzynski, 2014). To quantify ROS levels, conidiospores were harvested and adjusted in GB5 + 2% glucose medium to a final concentration of 10^5. Subsequently, 50 µl of conidial suspensions were placed in 96-well plates (Microplate pureGradeTM 96 well PS, transp. Bottom, black, Brand GmbH & Co KG, Germany) and incubated overnight. Just before taking fluorometric measurements the detection mix was added to the germinated conidia (1:10) and the Tecan Safire microplate reader (Tecan group Ltd., Switzerland) was used to detect ROS levels at the wavelengths 490/525 (Ex/Em). Fluorescence was measured at the bottom of the wells with at least 3 × 3 reads per well with the gain set to 200.

2.5. Confocal laser scanning microscopy (CLSM) imaging and ratiometric analysis

To monitor changes in the redox state indicated by roGFP2, an inverted microscope (Leica DMIRE2) equipped with a Leica TCS SP2 scan head (Leica Microsystems, Wetzlar, Germany) was used. Conidia were harvested and diluted to a final concentration of 10^5 conidia/ml in GB5 medium supplemented with 2% glucose as well as 1 mM $(NH_4)_2HPO_4$. After growth in darkness for 16 h, analyses were performed by using a 63× water-immersion lens in multi-track mode with line switching. Excitation wavelengths were set to 395 nm in the first track and 488 nm in the second track, while image collection took place with a 505–530 nm bandpass filter. Using the CLSM software Z-stacks of optical sections were collected and projected as average projections. Further calculation was done by the program ImageJ (v. 1.44f; http://rsb.info.nih.gov/ij/). For each image a Gaussian blur normalization with sigma of 2.0 was performed. To remove background pixels, the fluorescence intensity images were corrected. Subsequently, RatioPlus software was used to produce a ratio between the corrected 395 nm image and the corrected 488 nm image. Mean values were created with the 395/488 nm ratio with a clipping value of 2.0. For illustration, the threshold of intensity ratio images was set to 0–4. Finally the grayscale was changed to color using the look-up table "Fire" of the ImageJ program.

For fluorometric measurements, conidia were harvested from 7-day-old PDAB plates and incubated in malt medium (1.5%) for 12 h at 150 rpm. Before measurements, the spores were washed twice in GB5 medium, re-suspended in GB5 medium supplemented with 1 mM $(NH_4)_2HPO_4$ and 200 µl were placed in chambers of a 96-well plates (Microplate pureGradeTM 96 well PS, transp. Bottom, black, Brand GmbH & Co KG, Germany). Fluorescence was measured in a Tecan Safire reader (Tecan group Ltd., Switzerland) with 3 × 3 reads/well and excitation/emission wavelength as described above. The gain was set to 100. Relative fluorescence units were used to calculate the ratio between the two wavelengths.

2.6. Epifluorescence microscopy

To analyze samples by light microscopy the Axio Imager 2 (Zeiss, Jena, Germany) and the Axiovert (Zeiss, Jena, Germany) were used. For monitoring germinated conidia, 10 µl of a conidial suspension (1×10^5 conidia/ml) in GB5 medium supplemented with 10 mM glucose were dropped on to glass slides and incubated for 12–24 h. Analysis took place with 40× or 63× objective lens. To stain the ER, a 1:50 dilution of ER-Tracker™ Blue-White DPX (Life Technologies, Germany) in McIlvaine standard buffer (McIlvaine, 1921) was added to the germinating conidia. Subsequently the samples were observed via the filter set 49 DAPI shift free (excitation G 365, beam splitter FT 395, emission BP 445/50). The same method was used to visualize nuclei by Hoechst 33342 (Kangatharalingam and Ferguson, 1984). Staining of mitochondria was done by the MitoID red tracker (Enzo Lifescience, Germany) and detected with filter set 43 HE Cy 3 shift free (excitation BP 550/25, beam splitter FT 570, emission BP 605/70). GFP fluorescence was detected with filter set 38 (excitation BP 470/40, beam splitter FT 495, emission BP 525/50). Images were captured with a Zeiss AxioCamMRm camera and further analyzed using the AxiovisionRel 4.8 software package.

2.7. Database resources

Nucleotide and protein sequences of *B. cinerea* strain B05.10 was the *B. cinerea* database (http://fungi.ensembl.org/Botrytis_cinerea/Info/Index). The prediction of signal peptides was performed using the SignalP4.0 (http://www.cbs.dtu.dk/services/SignalP/) program (Petersen et al., 2011). Subcellular localization patterns of proteins were predicted by ProtComp v.9.0 (http://linux1.softberry.com/berry.phtml?topic=protcompan&group=help&subgroup=proloc); putative transmembrane domains were predicted according to the TMHMM method (http://www.cbs.dtu.dk/services/TMHMM/).

3. Results

3.1. Targeting of the biosensor roGFP2 to the mitochondria and the ER of B. cinerea

Genetically encoded fluorescent reporters (YFP- and GFP-based) have gained importance (Dooley et al., 2004; Østergaard et al., 2001) to visualize intracellular fluxes. One example is the redox sensitive GFP2 (roGFP2) that specifically displays the redox potential of the cellular glutathione pool. Depending on the redox environment, disulfide bonds are formed between additional cysteine residues located on two adjacent ß-strands in roGFP2, leading to conformational changes in the protein structure and therefore to an alteration in the protonation state of the fluorophore. The changes lead to different spectral properties with excitation wavelengths of 395 and 488 nm facilitating quantitative ratiometric imaging of redox dynamics (Dooley et al., 2004; Jiang et al., 2006; Morgan et al., 2011; Schwarzländer et al., 2008; Yu et al., 2009). The biosensor (cyt-roGFP2) was successfully expressed under control of a constitutive promoter (P*oli*C) in *B. cinerea,* and was applied as a tool to compare the cytosolic redox states in wild-type and mutant strains (Heller et al., 2012a, 2012b; Schumacher et al., 2014; Viefhues et al., 2014).

In consideration of the fact that the redox states in distinct cellular compartments may differ, we modified roGFP2 for specifically targeting it to the mitochondrial intermembrane space (IMS – in the following also stated as mitochondria) and the ER. For ER localization, the ER retention signal "HDEL" was fused to the C-terminus of roGFP2 (roGFP2_HDEL). Here essential processes such as the unfolded protein response or the oxidative protein folding (Tu et al., 2000) take place. Targeting the IMS was accomplished by adding the first 31 aa of cytochrome C (Bcin14g02370) to the N-terminus of roGFP2 (mito-roGFP2) (Fig. S1) (Sarewicz and Osyczka, 2015). The IMS is known as the action site of important proteins influencing the ROS homeostasis (respiratory chain), protein folding and the mitochondrial protein import machinery (Mesecke et al., 2005; Koehler and Tienson, 2009).

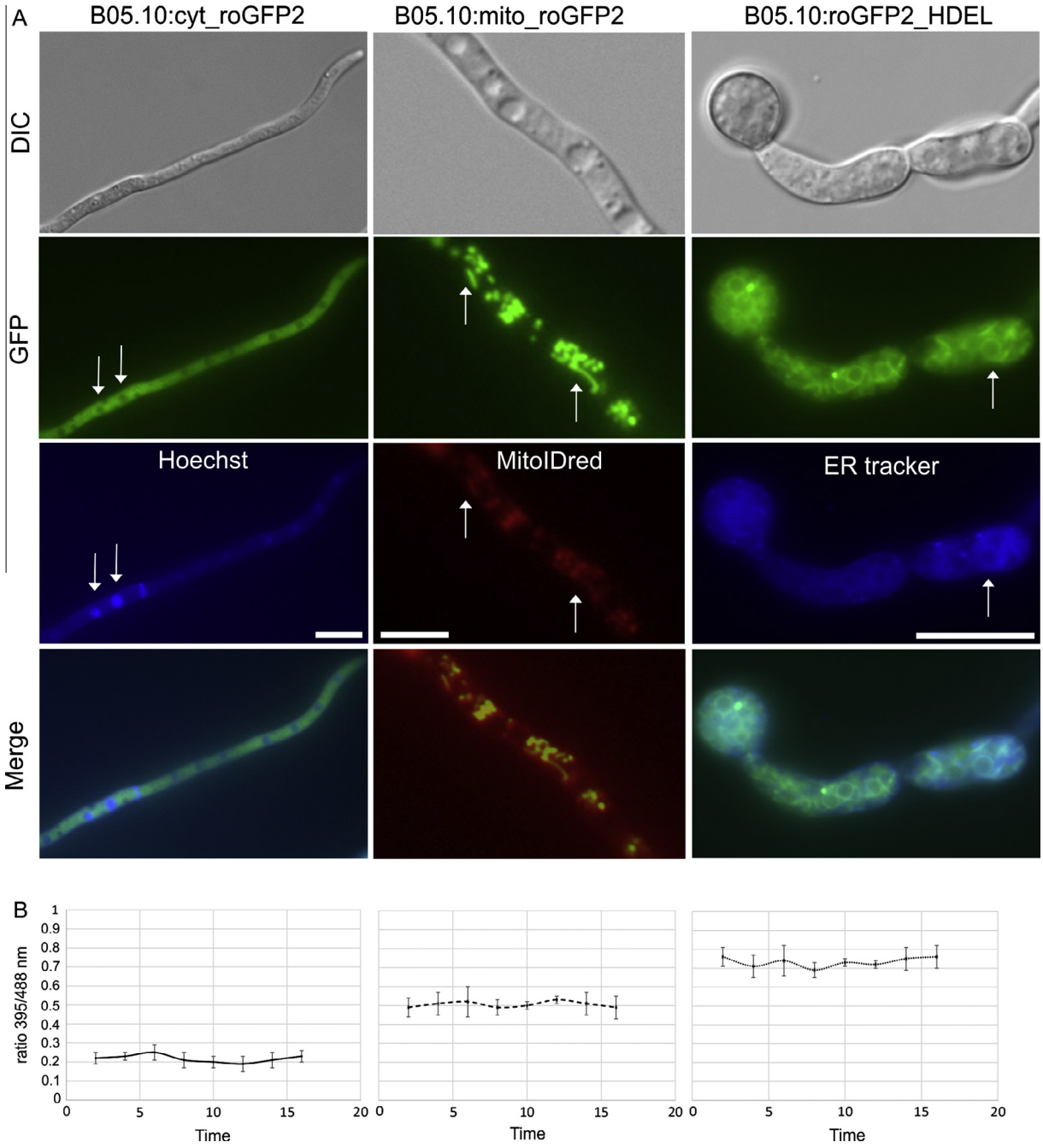

Fig. 1. (A) Localization of roGFP2 in different cellular compartments. The biosensor without and with targeting signals (first 31 aa of cytochrome C for mitochondrial targeting and HDEL for retention in the ER) under control of the constitutive P*oliC* was expressed in the wild type B05.10. For verification of cytosolic localization counter staining with Hoechst (staining of nuclei) was performed. Localization in mitochondria was checked by staining mitochondria with MitoID red. ER structures were stained with ER-Tracker™ Blue-White DPX. Scale bars = 20 µm, arrows indicating overlapping structures. (B) Redox states in the different compartments under non-stimulated conditions. Conidia were grown overnight on CLSM slides in B5 medium. Z-stack images were taken at 395/488 nm. Ratios were calculated from average projections. Mean values and standard deviations were calculated from three independent biological replicates.

The constructs were introduced in the wild type B05.10 and the correct targeting to the ER and mitochondria was verified microscopically via co-staining with ER-Tracker™ Blue-White DPX and the MitoID red coloring agent (Fig. 1A). Growth rates, germination rates, penetration abilities and virulence of the roGFP2-expressing strains confirmed that the integration of the biosensor in the different compartments had no influence on the phenotype (data not shown). To study the role of the two catalytic subunits of the Nox complexes (NoxA, NoxB), the thioredoxin Trx1 and the transcription factor Ltf1 for regulating the redox states in different compartments, the newly generated roGFP2 constructs were expressed in the respective deletion mutants (Table S2). The confocal data reported here were confirmed by fluorometric measurement in a 96-well format (Table S6).

3.2. The redox states in the cytosol, mitochondria and the ER differ

In a previous study, it was shown that the cytosol of *B. cinerea* is oxidized and reversibly influenced by the addition of the oxidant H_2O_2 and the reducing agent 1,4-dithiothreitol (DTT) (Heller et al., 2012a, 2012b). Measurements of the glutathione pool (here referred to as redox state) of unstimulated hyphae of the wild type

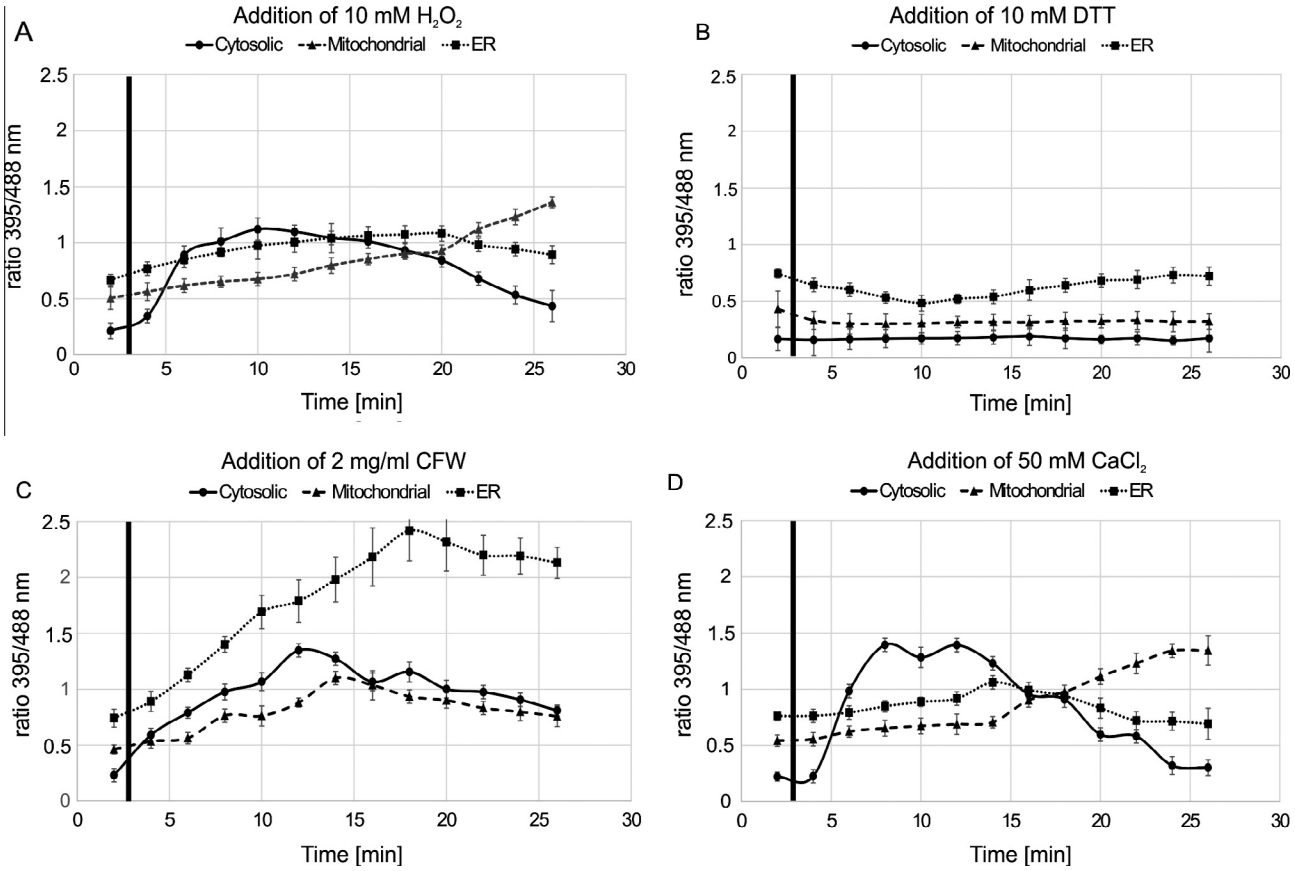

Fig. 2. Redox states in the different cellular compartments after exposure to stress-inducing agents. Conidia were harvested and grown overnight on a microscopic slide (CLSM) in B5 medium. Z-stacks images were taken by CSLM with excitation wavelengths at 395 and 488 nm. Average projections and ratios between the values at 395 nm (oxidized state) and 488 nm (reduced state) were calculated. After the first measurement at 2 min, control medium (GB5) was removed and replaced by stress-inducing agents (black bars). The effect of H_2O_2 (A), DTT (B), calcofluor white (CFW) (C) and calcium chloride ($CaCl_2$) (D) was monitored until 24 min post induction. For every experiment the ratio of four hyphae was evaluated. Mean values and standard deviations are shown. As negative control, GB5 medium was added; no alteration of the redox states were observed (data not shown).

revealed that mitochondria are compartments with a higher oxidation state than the cytosol. The ratio between the resulting CSLM images (excitation 395/488 nm) was 0.2–0.3 in the cytosol while in the IMS ratios of 0.5–0.6 were calculated. However, the most oxidized compartment was the ER with a ratio of 0.8–0.9 (Fig. 1B). Similar values were obtained for the respective deletion mutants, suggesting that neither the Nox complexes nor BcLtf1 and BcTrx1 have an influence on the general redox states under non-stimulated conditions.

3.3. The subcellular redox states changes upon exogenous stress

To verify the functionality of the constructs and to chase stress signals in the different cellular compartments, hyphae of the different strains were grown overnight in droplets of GB5 medium on microscopic CLSM slides and then exposed to 10 mM H_2O_2, 10 mM DTT, 50 mM calcium chloride ($CaCl_2$), 1 mg/ml calcofluor white (CFW) and GB5 as a negative control medium, respectively. H_2O_2 led to an increase of the $_{395/488}$ratio in the cytoplasm indicating a more oxidized state, as previously described (Heller et al., 2012a, 2012b). The maximum was reached after 10 min of exposure. In contrast, the mitochondrial redox state changed in the first 20 min only slightly ($_{395/488}$ratio of 0.5–0.9), then a significant oxidation was observed (0.9–1.4). Interestingly, while in the cytosol the decrease of the $_{395/488}$ratio to the ground level was monitored within the observed time frame there was no shift to the basis in mitochondria. The redox state of the ER was also slightly influenced by the addition of H_2O_2; the $_{395/488}$ratio changed from 0.7 to 1.05 within the first 20 min. Afterwards a decrease in the $_{395/488}$ratio was observed indicating the restoration of the initial environment (Fig. 2A).

The addition of the reducing agent DTT did not affect cytosolic and mitochondrial redox states, while the $_{395/488}$ratio of the ER was slightly diminished (0.75–0.48) within 10 min. Here, a rapid regeneration to the basic level was monitored (Fig. 2B). Due to its minor effect, we excluded DTT from further experiments.

The addition of the cell wall-interfering agent CFW led to a rapid increase of the $_{395/488}$ratio in every compartment. However, the local maxima differed: after 12 min in the cytosol, after 14 min in the mitochondria and after 18 min in the ER. In all compartments the glutathione pool started to regenerate within the observed time frame (Fig. 2C). Surprisingly, the redox state of the ER shifted to a more oxidized one after the addition of CFW (ratio: 2.45) than seen for H_2O_2 (ratio: 1.05).

The addition of $CaCl_2$ as inducer of calcium stress resulted in a similar pattern as the addition of H_2O_2 (Fig. 2D). The cytosol became rapidly oxidized (maximum of 1.4 after 8 min); a change in the mitochondrial redox state could be detected starting 12 min after $CaCl_2$ addition. The $_{395/488}$ratio inside of the ER was only slightly influenced (0.77–1.05).

In response to H_2O_2, $CaCl_2$ and CFW, the redox state changed in the cytosol first and then in mitochondria and ER. Taken together, the experiments demonstrated that all different stressors led to changes in the cellular redox state, but the glutathione pool in the three cellular compartments responded differentially to these exogenously applied stressors: the addition of $CaCl_2$ and H_2O_2

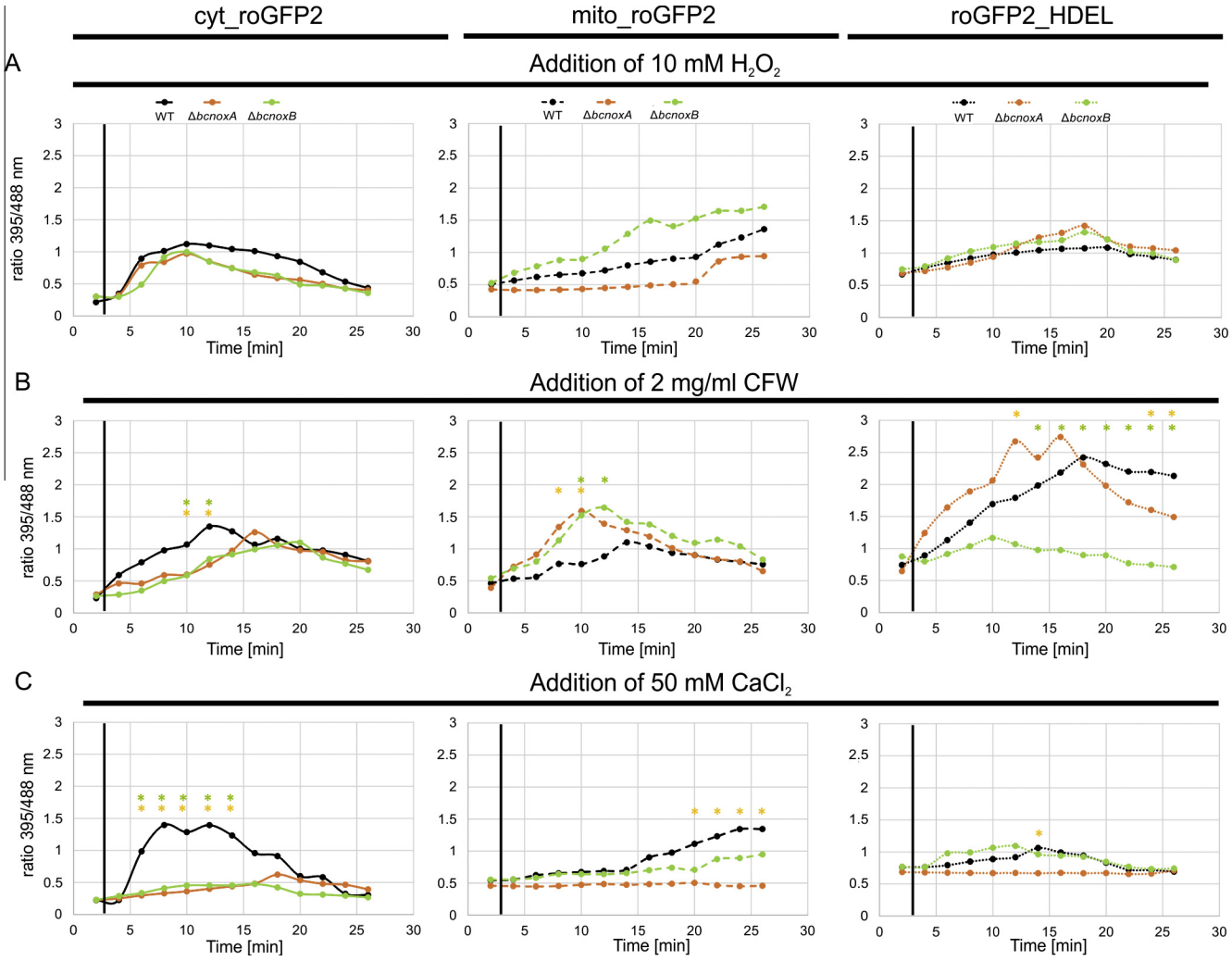

Fig. 3. Comparison of cytosolic, mitochondrial and ER redox states of wild type B05.10 and Δ*bcnoxA* and Δ*bcnoxB* mutants under stress-inducing conditions. Z-stacks images were taken by CSLM with excitation wavelengths of 395 and 488 nm. Average projections were calculated. The ratio between both channels was formed. The stress-inducing agents H_2O_2 (A), CFW (B) and $CaCl_2$ (C) were added after 3 min (black bars). Mean values and standard deviations (depicted in Table S2) were calculated from four different experiments. Asterisks indicate significant differences to the wild-type control in every condition (*t*-test, $P < 0.01$).

rapidly led to a more oxidized cytosol, while the exposure to cell wall stress (CFW/Congo red) (Figs. 2C and S7) had its main effect on the redox state in the ER.

3.4. The catalytic subunits BcNoxA and BcNoxB have specific effects on redox homoeostasis

Since Nox complexes are major producers of ROS; they transfer electrons from the cytosol across the respective membranes, regularly on to molecular oxygen. To check their influence on the intracellular redox state, the redox states in corresponding deletion mutants (Δ*bcnoxA*, Δ*bcnoxB*) were investigated. BcNoxA and BcNoxB are the catalytic subunits of two distinct complexes which were shown to be involved in mostly independent processes (Roca et al., 2012; Segmueller et al., 2008; Siegmund et al., 2013, 2015). In *B. cinerea*, both Nox complexes are located in membrane structures of the ER and the plasma membrane (Siegmund et al., 2013).

Although both deletion mutants are more sensitive to oxidative stress than the wild type (Siegmund et al., 2013, 2015), the addition of H_2O_2 led to a wild-type-like pattern of the $_{395/488}$ratio in every compartment (Fig. 3A/Table S4). No significant differences were observed.

Instead, the cytosolic redox state of both mutants did not change upon exposure to $CaCl_2$. While the $_{395/488}$ratio immediately increased after addition of calcium stress in the wild type, the cytosolic glutathione pool of both mutants stayed unaffected. Moreover, the $_{395/488}$ratio in mitochondria and the ER of Δ*bcnoxA* did not change after the addition of calcium, although the $_{395/488}$ratio in the wild type was also increased (Fig. 3C).

The addition of CFW as inducer of cell wall stress led to an oxidation of all compartments. In the cytosol, the mutants displayed a similar pattern as the wild type. However, the local maximum of the $_{395/488}$ratio was slightly shifted (WT after 10 min post induction, Δ*bcnoxA* after 14 min; Δ*bcnoxB* after 18 min). On the contrary, the $_{395/488}$ratio in mitochondria increased faster in both deletion mutants (peak in the wild type 12 min post induction; Δ*bcnoxA* after 8 min; Δ*bcnoxB* after 10 min) and reached higher values (~1.5) than in the wild type (1.05). Within the ER, the deletion mutant of *bcnoxA* behaved similarly to the wild type, while the effect on the glutathione pool in the *bcnoxB* mutant was significantly attenuated (Fig. 3B).

In summary, both Nox complex mutants are affected in subcellular redox states. Although both Nox subunits are involved in the resistance to oxidative stress and in the production of endogenous ROS, the redox state of both mutants did not change differentially

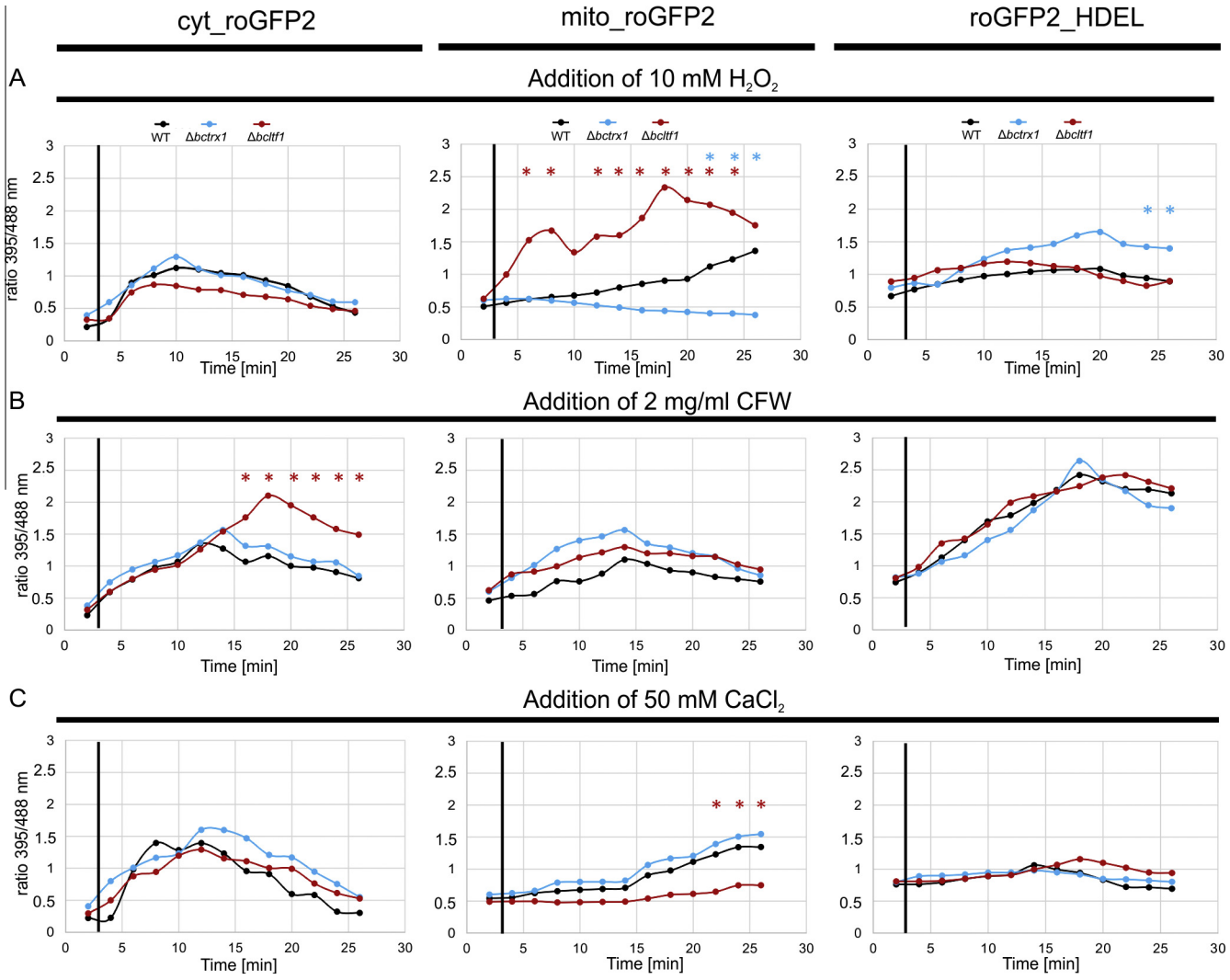

Fig. 4. Cytosolic, mitochondrial and ER redox states of Δ*bcltf1* and Δ*bctrx1* mutants compared to wild type B05.10 after the addition of stress-inducing agents. Z-stacks images were taken by CSLM with excitation wavelength of 395 and 488 nm. The ratio between average projections of both channels was formed. The stress-inducing agents were added after 3 min (black bars). The cytosolic (left), mitochondrial (centered) and ER (right) redox states of the wild type and the deletion mutants of *bcltf1* and *bctrx1* were monitored under the influence of H_2O_2 (A), CFW (B) and $CaCl_2$ (C). Mean values and standard deviations (depicted in Table S5) were calculated from four independent experiments. Asterisks indicate significant differences to the wild-type control in every condition (*t*-test, $P < 0.01$).

to the wild type upon exposure to H_2O_2. But the redox changes induced by cell wall stress and especially Ca^{2+} depend on functional Nox complexes.

3.5. BcLtf1 has impact on the mitochondrial redox state

Deletion mutants of the light-responsive transcription factor 1 (BcLtf1) were investigated using the newly developed biosensors since a role of the TF in maintenance of cellular redox states was proposed in a previous study. The transcription factor has an exceptional function in *B. cinerea*; it is, for instance, required for growth in (excessive) light, to cope with oxidative stress and for virulence. Moreover, the deletion mutants produce more ROS and some of the phenotypes could be restored by applying antioxidants (Schumacher et al., 2014). As previously shown, the cytosolic glutathione pool is oxidized upon exposure to H_2O_2 in a wild-type-like manner; a similar pattern was found in this study for the redox state of the ER (Fig. 4/Table S5). However, the mitochondrial redox state shifted to a more oxidized state immediately after addition of the oxidant (from 0.62 to 2.32 after 16 min post induction); and no recovery of the initial situation was observed within the studied time frame. A similar, but opposite effect was observed after the addition of $CaCl_2$: the shift of the $_{395/488}$ratio in mitochondria to higher values was attenuated in Δ*bcltf1*.

In response to cell wall stress, the $_{395/488}$ratios in the mitochondria and the ER were not significantly altered. However, the cytosolic glutathione pool was shifted to a more oxidized state (maximum: 2.05 after 16 min) than in the wild type (maximum: 1.35 after 10 min).

Taken together, these experiments confirmed the assumed role of the TF in maintaining the cellular redox states and its postulated effect on mitochondrial respiration (Schumacher et al., 2014). The mitochondrial redox state is influenced after applying oxidative and calcium stress most markedly and in an opposing manner whereby hyper-oxidation and no oxidation occurred in response to H_2O_2 and $CaCl_2$.

3.6. The thioredoxin BcTrx1 is involved in regulation of the redox state

Finally, redox changes in the deletion mutant of *bctrx1* were monitored. BcTrx1, which is involved in oxidative stress resistance and virulence, was localized in the cytosol (Viefhues et al., 2014).

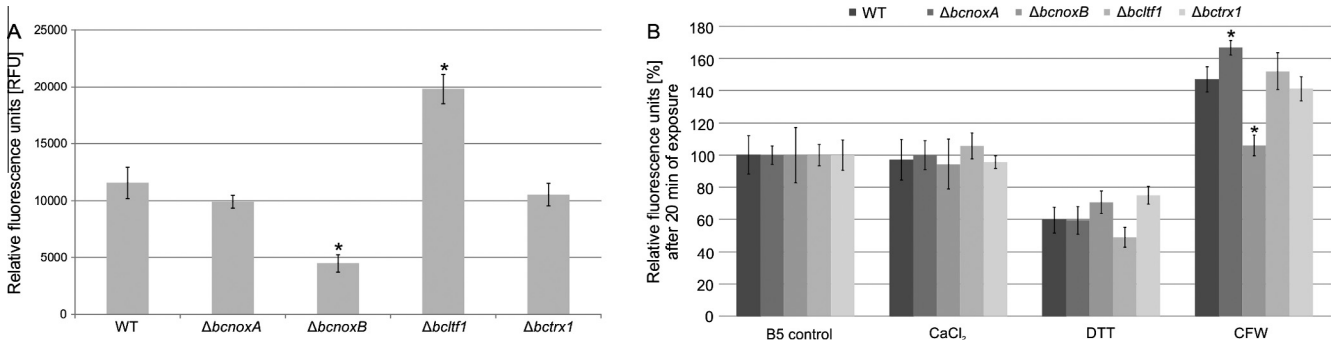

Fig. 5. ROS production of Δ*bcnoxA*, Δ*bcnoxB*, Δ*bctrx1* and Δ*bcltf1* mutants compared to wild type B05.10 (A) ROS accumulation in the strains under non-stressed conditions. Conidia (10^5) were cultivated overnight in GB5 medium in a 96-well plate. 20 min after addition of 1/10 vol. of the ROS detection agent fluorescence was quantified [RFU]. (B) ROS accumulation in the strains after exposure to stress-inducing agents. Besides 1/10 vol. of the detection agent, 1 vol. of the appropriate stress-inducing agent was added to the wells. After 20 min of addition of the ROS detection agent and stress-inducing agent, the quantity of ROS was calculated fluorometrically. The values obtained in the B5-control (addition of 1 vol. GB5 medium) were set to 100%. Asterisks indicate significant differences between the wild type and the respective mutants ($P < 0.01$).

Nevertheless, addition of H_2O_2 had no influence on the cytosolic redox state, whereas the ER was much more oxidized (maximum: 1.68 after 18 min) than in the wild type (maximum: 1.06 after 18 min post induction). The $_{395/488}$ratios in mitochondria was reduced upon exposure to oxidative stress from 0.54 to 0.37 compared to the wild type (0.50–1.38) (Fig. 4A/Table S6). The addition of CFW as well as $CaCl_2$ did not have any specific influence on the cytosolic, mitochondrial and ER redox states of the mutant.

3.7. BcNoxB and BcLtf1, but not BcNoxA and BcTrx1, are involved in ROS production

To elucidate whether the different impacts of exogenous stressors on the mutants' redox states are associated with altered properties of the mutants to produce ROS, we used the ROS/superoxide detection kit (TRD-kit), allowing the exact quantification of ROS (Marschall and Tudzynski, 2014). Conidia (10^5) were cultivated overnight in a 96-well plate and immediately prior to measurement 1/10 vol. of detection mix was added to the medium.

While Δ*bctrx1* produced similar amounts of ROS as the wild type, Δ*bcltf1* displayed significantly increased ROS levels, indeed twice as high as the wild type (Fig. 5A). These results confirm observations previously made by use of the less precise 3,3′-diaminobenzidine (DAB) assay (Schumacher et al., 2014; Viefhues et al., 2014). Δ*bcnoxB* mutants produced significantly less ROS than the wild type, whereas the ROS level was only slightly reduced in *bcnoxA* mutants, suggesting that the NoxB complex is responsible for most of the Nox-dependent ROS production and secretion.

3.8. CFW, but not $CaCl_2$ trigger ROS production in B. cinerea

The stress-inducing agents that were used in the roGFP2 experiments were also tested with regard to their effect on the ROS production. H_2O_2 was excluded from these experiments, because it was found that the addition led to an immediate increase of the relative fluorescence units above the detection maximum (concentrations of 10–1 mM were tested).

The ROS production (measured after 20 min of exposure) in the wild type was significantly altered upon exposure to DTT (reduced) and CFW (increased), but not in response to $CaCl_2$ (Fig. 5B).

In response to $CaCl_2$ and DTT wild-type-like results for all mutants were obtained. However, both Nox mutants differed in their stress response to CFW: while Δ*bcnoxB* mutants were unaffected, the Δ*bcnoxA* mutant produced even significantly higher amounts of ROS than the wild type under these conditions.

4. Discussion

The elucidation of ROS as signaling molecules within complex cascades and the intracellular connection of signaling pathways is a major goal of current research in fungi. In *B. cinerea*, production of ROS during plant pathogen interactions (Govrin and Levine, 2000) as well as during intracellular differentiation processes, such as appressoria formation, are tightly controlled (Marschall and Tudzynski, 2014). There are several, already analyzed proteins which are known to affect the ROS homeostasis or the resistance towards oxidative stress such as mutants deleted for MAP kinases (Heller et al., 2012a, 2012b), Nox subunits (Siegmund et al., 2013, 2015) and antioxidative enzymes (Viefhues et al., 2014). Most of them are additionally contributing to virulence suggesting an important role of the fungal redox state in the interaction with the host.

For a deeper insight into the role of the redox state and the equilibrium between ROS production and scavenging, the genetically encoded biosensor roGFP2 was modified for the visualization of the redox state (in more detail: the glutathione pool) in the cytosol (Heller et al., 2012a, 2012b), the ER and the intermembrane space (IMS) of mitochondria.

The cellular compartments were differentially oxidized when unstimulated. While the mitochondrial IMS was slightly more oxidized than the cytosol, the ER was the most oxidized compartment. These results fit with observations in *Arabidopsis thaliana*, where similar results were obtained (Schwarzländer et al., 2008, 2009). The ER as well as the IMS of mitochondria have to be more oxidized in order to allow oxidative protein folding that takes place in both compartments (Koehler and Tienson, 2009; Tu et al., 2000). Surprisingly, the glutathione pool of the ER could be further oxidized by the addition of stress-inducing agents, especially by CFW. This finding is opposite to the situation in *A. thaliana*: in the model plant, the ER appeared fully oxidized (Meyer et al., 2007; Schwarzländer et al., 2008).

To elucidate the effect of stress-inducing agents on the redox state in *B. cinerea*, conidia were exposed to oxidative (H_2O_2), calcium ($CaCl_2$) and cell wall (CFW) stress. In contrast to the cytosolic redox state of the wild type that is quickly shifted to a more oxidized state by the addition of H_2O_2 (Heller et al., 2012a, 2012b), the redox states of the mitochondria and the ER are only marginally affected by exposure to H_2O_2 in a time-dependent manner (Fig. 2A). The mitochondrial IMS is slightly oxidized when the cytosolic redox state is already recovering to the basic state suggesting an interdependency of the glutathione pools in both compartments. A tight connection between the cytosolic redox state and the IMS has been described in mammalian cell lines (Kojer

et al., 2012) where porins were shown to be responsible for the dynamic balance between cytosolic and IMS redox states mediated by the glutathione reductase system. Another reason for the delayed response of the IMS to oxidative stress may due to different scavenging capacities. The observation that the addition of H_2O_2 impacts the redox state of the ER only marginally may indicate that H_2O_2 cannot enter the ER or that the glutathione pool differs in its buffer capacity.

As the production of ROS in plants occurs in response to the increase of cytosolic Ca^{2+} levels (Gilroy et al., 2014), we analyzed the effect of exogenous Ca^{2+} in form of $CaCl_2$ on the redox states in the different compartments. The addition of $CaCl_2$ has previously been shown to trigger fast responses in *B. cinerea*: it causes the rapid translocation (within 10 min) of the Ca^{2+}/calcineurin-dependent TF BcCRZ1 from the cytosol to the nuclei (Schumacher, 2012) and changes in the genome-wide gene expression pattern (B. Brandhoff, J. Schumacher, A. Simon, M. Viaud, B. Tudzynski, unpublished). As shown in this present study, the exposure to Ca^{2+} has impact on the cytosolic redox state – a "burst" (oxidation) was observed after 8 min of Ca^{2+} addition, suggesting that an increase of cytosolic Ca^{2+} stimulates the production of ROS. In accordance with the minor effect of H_2O_2 on the redox states of the mitochondria and the ER, the exposure to Ca^{2+} has only slight effects in these compartments. The mitochondrial glutathione pool became more oxidized after 16 min – at this time, the cytosolic redox state had already recovered. The oxidative effect of Ca^{2+} could perhaps be ascribed to two different signaling pathways. The massive Ca^{2+} influx may lead to the induction of apoptotic processes (Orrenius et al., 2003), which are tightly associated with the oxidation of glutathione (Circu and Aw, 2010). Another possibility is the activation of ROS-producing enzymes, as previously described in plant cells (Gilroy et al., 2014). Therefore, plant protein kinases are able to activate members of the NADPH oxidase (NOX) complex as a downstream target (Dubiella et al., 2013; Drerup et al., 2013). In fungi, elevated Ca^{2+} levels are sensed by Ca^{2+}-binding proteins such as calmodulin (CaM) and this leads to the activation of Ca^{2+}-regulated enzymes such as the protein kinase C (PKC), Ca^{2+}/CaM-dependent kinases and the calcineurin phosphatase (CN) and, thus, TF BcCrz1 (reviewed in Thewes, 2014). In *B. cinerea*, CN and its downstream target BcCrz1 were shown to facilitate growth in the presence of H_2O_2 and Ca^{2+} (Schumacher et al., 2008; Harren et al., 2012) leading to the assumption that Ca^{2+}- and ROS-dependent signaling pathways are connected.

Besides H_2O_2 and $CaCl_2$, CFW had a profound effect on the redox state of all studied compartments. The impact of cell wall stress may be indirect. The cell wall-interfering agent might trigger the unfolded protein response via the cell wall integrity pathway (Krysan, 2009) and thus might be responsible for ROS production and an oxidized ER lumen (Santos et al., 2009). Additionally, the cell wall stress may be mediated via Ca^{2+} signaling pathways. Thus, it is known that PKC is highly involved in cell wall integrity (Heinisch et al., 1999), the calcineurin pathway triggers cell wall maintenance and calcium channels appear to control cell wall synthesis (Bormann and Tudzynski, 2009).

In conclusion, the redox state of the different fungal compartments is affected by the stress-inducing agents in different ways and in a temporally shifted manner. Surprisingly, every stress signal seems to be transduced into a changed redox potential. Similar results were previously obtained for redox changes induced by osmotic stress agents in *Fusarium graminearum* (Mentges and Bormann, 2015).

A protein which is required for full virulence of *B. cinerea* and involved in the regulation of oxidative stress responses (Viefhues et al., 2014) is the small redox protein Trx1. The protein has an antioxidative role (Lu and Holmgren, 2014) and thus might be involved in the maintenance of the redox state. In contrast to the wild type, the redox states of Δ*bctrx1* only differently change upon exposure to oxidative stress. Surprisingly, H_2O_2 affects the redox state of the ER and the IMS, although the protein was shown to be located inside the cytosol (Viefhues et al., 2014). However, bioinformatic analyses suggest also targeting of BcTrx1 to the mitochondria. Similar results were observed in plants and higher eukaryotes (Laloi et al., 2001; Benhar et al., 2008). The lack of effect of $CaCl_2$ and CFW in this system may be caused by several factors. On the one hand, BcTrx1 might not be involved in the regulation of Ca^{2+} and cell wall stress; on the other hand additional thioredoxins or thioredoxin-like proteins may compensate the loss of BcTrx1, as previously shown in other organisms (Malagnac et al., 2007; Meyer et al., 2009).

By expressing the different roGFP2 versions in the mutants of the catalytic subunits of the Nox complexes, we aimed to elucidate, how the Nox complexes are linked to other signaling pathways and where the Nox complexes have their site of action. Both catalytic subunits are located at the ER- and the plasma membrane and at least BcNoxA has a distinct function inside the ER (Siegmund et al., 2015). Additionally, they are transcriptionally regulated by MAPK kinases (Segmueller et al., 2008), and corresponding deletion mutants are sensitive towards oxidative stress (Siegmund et al., 2013, 2015). By roGFP2 measurements, we demonstrated that both BcnoxA and BcnoxB are required for the fast oxidation of the cytosolic glutathione pool ("burst") upon exposure to $CaCl_2$. From these data, we conclude that the observed "bursts" are achieved by the activity of the Nox subunits, i.e. that the subunits may be activated by Ca^{2+} as shown for Nox subunits in plants and mammals (Lambeth, 2004), resulting in the electron transfer and consequently the oxidation of the cytosol. However, the fact that the attenuation was detected in both Nox single mutants is striking and would imply an interdependency of the two Nox complexes. This apparently contradicts previous results that reveal distinct functions for both Nox complexes and that the catalytic subunits cannot replace each other (Siegmund, Marschall and Tudzynski, unpubl.). A possible scenario might be the serial activation of both subunits in response to a Ca^{2+} stimulus. BcNoxB might be (in this case) the predominant one, since a severe reduction of the total ROS accumulation in Δ*bcnoxB* mutants was found (Fig. 5A). Instead, the NoxA complex might be responsible for the smooth regulation of intracellular processes (predominantly inside of the ER membrane) by producing only small and locally limited amounts of total H_2O_2.

Surprisingly, the addition of H_2O_2 led to a nearly wild-type-like redox state pattern. These data suggests that oxidative stress induced by H_2O_2 does not activate Nox complex activity inside of the ER, or at the plasma membrane, although both catalytic subunits are involved in stress resistance to oxidative stress (Segmueller et al., 2008; Siegmund et al., 2013, 2015). However, the redox states in the IMS differ slightly. While the deletion of *bcnoxA* led to an attenuated change of the redox state, the deletion of *bcnoxB* had the opposite effect (Fig. 3A). This effect upon stimulation with H_2O_2 may be due to an indirect effect of the deletion since ROS production and scavenging capacities were generally diminished in the mutants, rather due to a direct effect as Nox-complexes are absent from mitochondria in fungi.

As discussed above, the different responses to H_2O_2 in the distinct compartments may be due to differences in the presence and efficiency of the scavenging systems. *Bctlf1* deletion mutants generally show poor growth and they cannot cope with (additional) oxidative stress which arises during exposure to exogenous ROS, excessive light provoking the formation of singlet oxygen, and the plants' oxidative burst. Expression data indicated the upregulation of genes encoding components of the alternative respiration pathway (retrograde response), e.g. the alternative oxidase (AOX)

which facilitates the electron flux without generation of additional ROS. The monitoring of the cytosolic roGFP2 after addition of H_2O_2 did not reveal significant differences compared to the wild type, leading to the hypothesis that the Δ*bcltf1* mutant experiences oxidative stress in another compartment, for instance in the mitochondria (Schumacher et al., 2014). Expressing the new versions of roGFP2 in the Δ*bcltf1* mutant, we finally could confirm the dysfunction of the mitochondria in coping with additional oxidative stress. Though the basic redox states in the mitochondria were comparable with those in the wild type, the addition of H_2O_2 caused the massive and stable oxidation of the glutathione pool. In contrast, the redox states in the other studied compartments were not significantly affected underlining furthermore the fact that the redox states of the compartments are predominantly and independently controlled and may differ due to different buffer capacities.

5. Conclusion

We expressed the biosensor roGFP2 in different cellular compartments of *B. cinerea,* for the first time in a filamentous fungus, and showed that the redox state is gradually shifted from the cytosol to mitochondria and the ER as the most oxidized compartment. We present evidence that different external stressors have impact on the redox states of the three compartments; they are first recognized and transmitted in the cytosol and afterwards in the ER or the mitochondrial intermembrane space. Moreover, our data underline the close association of ROS, Ca^{2+} signaling and cell wall stress. The compartment-specific redox state in the Nox deletion mutants is not differentially influenced by oxidative stress compared to the wild type. But while exposure to $CaCl_2$ and cell wall stress leads to a "burst" in the wild type, the redox states of both deletion mutants appear completely unaffected.

Acknowledgments

We thank Brian Williamson for critical reading of the manuscript and Bettina Richter for excellent technical assistance, Anne Dornieden for discussion and providing the mutant Δ*bctrx1,* and the DFG (Tu 50/19) for funding.

Appendix A. Supplementary material

Supplementary data associated with this article can be found, in the online version, at http://dx.doi.org/10.1016/j.fgb.2016.02.006.

References

Apel, K., Hirt, H., 2004. Reactive oxygen species: metabolism, oxidative stress, and signal transduction. Annu. Rev. Plant Biol. 55, 373–399.
Appenzeller-Herzog, C., 2011. Glutathione- and non-glutathione-based oxidant control in the endoplasmic reticulum. J. Cell Sci. 124 (Pt 6), 847–855.
Arner, E.S., Holmgren, A., 2000. Physiological functions of thioredoxin and thioredoxin reductase. Eur. J. Biochem. 267, 6102–6109.
Beckman, K.B., Ames, B.N., 1998. The free radical theory of aging matures. Physiol. Rev. 78, 547–581.
Benhar, M., Forrester, M.T., Hess, D.T., Stamler, J.S., 2008. Regulated protein denitrosylation by cytosolic and mitochondrial thioredoxins. Science 320, 1050–1054.
Bormann, J., Tudzynski, P., 2009. Deletion of Mid1, a putative stretch-activated calcium channel in *Claviceps purpurea*, affects vegetative growth, cell wall synthesis and virulence. Microbiology 155, 3922–3933.
Buettner, P., Koch, F., Voigt, K., Quidde, T., Risch, S., Blaich, R., Bruckner, B., Tudzynski, P., 1994. Variations in ploidy among isolates of *Botrytis cinerea*: implications for genetic and molecular analyses. Curr. Genet. 25, 445–450.
Cano-Dominguez, N., Alvarez-Delfin, K., Hansberg, W., Aguirre, J., 2008. NADPH oxidases NOX-1 and NOX-2 require the regulatory subunit NOR-1 to control cell differentiation and growth in *Neurospora crassa*. Eukaryot. Cell 7, 1352–1361.
Cenis, J.L., 1992. Rapid extraction of fungal DNA for PCR amplification. Nucl. Acids Res. 20, 2380.
Circu, M.L., Aw, T.Y., 2010. Reactive oxygen species, cellular redox systems, and apoptosis. Free Radic. Biol. Med. 48, 749–762.
Dalmais, B., Schumacher, J., Moraga, J., Le Pecheur, P., Tudzynski, B., Collado, I.G., Viaud, M., 2011. The *Botrytis cinerea* phytotoxin botcinic acid requires two polyketide synthases for production and has a redundant role in virulence with botrydial. Mol. Plant. Pathol. 12, 564–579.
Dean, R., Van Kan, J.A., Pretorius, Z.A., Hammond-Kosack, K.E., Di Pietro, A., Spanu, P. D., Rudd, J.J., Dickman, M., Kahmann, R., Ellis, J., Foster, G.D., 2012. The Top 10 fungal pathogens in molecular plant pathology. Mol. Plant Pathol. 13, 414–430.
Doehlemann, G., Berndt, P., Hahn, M., 2006. Trehalose metabolism is important for heat stress tolerance and spore germination of *Botrytis cinerea*. Microbiology 152 (Pt 9), 2625–2634.
Dooley, C.T., Dore, T.M., Hanson, G.T., Jackson, W.C., Remington, S.J., Tsien, R.Y., 2004. Imaging dynamic redox changes in mammalian cells with green fluorescent protein indicators. J. Biol. Chem. 279, 22284–22293.
Drerup, M.M., Schlucking, K., Hashimoto, K., Manishankar, P., Steinhorst, L., Kuchitsu, K., Kudla, J., 2013. The Calcineurin B-like calcium sensors CBL1 and CBL9 together with their interacting protein kinase CIPK26 regulate the *Arabidopsis* NADPH oxidase RBOHF. Mol. Plant 6, 559–569.
Dubiella, U., Seybold, H., Durian, G., Komander, E., Lassig, R., Witte, C.P., Schulze, W. X., Romeis, T., 2013. Calcium-dependent protein kinase/NADPH oxidase activation circuit is required for rapid defense signal propagation. Proc. Natl. Acad. Sci. USA 110, 8744–8749.
Egan, M.J., Wang, Z.Y., Jones, M.A., Smirnoff, N., Talbot, N.J., 2007. Generation of reactive oxygen species by fungal NADPH oxidases is required for rice blast disease. Proc. Natl. Acad. Sci. USA 104, 11772–11777.
Elad, Y., Williamson, B., Tudzynski, P., Delen, N., 2007. *Botrytis* spp. and diseases they cause in agricultural systems – an introduction. In: Elad, Y., Williamson, B., Tudzynski, P., Delen, N. (Eds.), *Botrytis*: Biology, Pathology and Control. Springer, Netherlands, pp. 1–8.
Elad, Y., Pertot, I., Cores-Prado, A.M., Stewart, A., 2016. Plant hosts of *Botrytis* spp. In: Fillinger, S., Elad, Y. (Eds.), Botrytis – the Fungus, the Pathogen and its Management in Agricultural Systems. Springer Verlag, http://dx.doi.org/10.1007/978-3-319-23371-0.
Gilroy, S., Suzuki, N., Miller, G., Choi, W.G., Toyota, M., Devireddy, A.R., Mittler, R., 2014. A tidal wave of signals: calcium and ROS at the forefront of rapid systemic signaling. Trends Plant Sci. 19, 623–630.
Gonzalez Porque, P., Baldesten, A., Reichard, P., 1970. The involvement of the thioredoxin system in the reduction of methionine sulfoxide and sulfate. J. Biol. Chem. 245, 2371–2374.
Govrin, E.M., Levine, A., 2000. The hypersensitive response facilitates plant infection by the necrotrophic pathogen *Botrytis cinerea*. Curr. Biol. 10, 751–757.
Gronover, C.S., Kasulke, D., Tudzynski, P., Tudzynski, B., 2001. The role of G protein alpha subunits in the infection process of the gray mold fungus *Botrytis cinerea*. Mol. Plant Microbe Interact. 11, 1293–1302.
Harren, K., Schumacher, J., Tudzynski, B., 2012. The Ca^{2+}/calcineurin-dependent signaling pathway in the gray mold *Botrytis cinerea*: the role of calcipressin in modulating calcineurin activity. PLoS ONE 7, e41761.
Heinisch, J.J., Lorberg, A., Schmitz, H.P., Jacoby, J.J., 1999. The protein kinase C-mediated MAP kinase pathway involved in the maintenance of cellular integrity in *Saccharomyces cerevisiae*. Mol. Microbiol. 32, 671–680.
Heller, J., Meyer, A.J., Tudzynski, P., 2012a. Redox-sensitive GFP2: use of the genetically encoded biosensor of the redox status in the filamentous fungus *Botrytis cinerea*. Mol. Plant Pathol. 8, 935–947.
Heller, J., Ruhnke, N., Espino, J.J., Massaroli, M., Collado, I.G., Tudzynski, P., 2012b. The mitogen-activated protein kinase BcSak1 of *Botrytis cinerea* is required for pathogenic development and has broad regulatory functions beyond stress response. Mol. Plant Microbe Interact. 25, 802–816.
Hwang, C., Sinskey, A.J., Lodish, H.F., 1992. Oxidized redox state of glutathione in the endoplasmic reticulum. Science 257, 1496–1502.
Jiang, K., Schwarzer, C., Lally, E., Zhang, S., Ruzin, S., Machen, T., Remington, S.J., Feldman, L., 2006. Expression and characterization of a redox-sensing green fluorescent protein (reduction-oxidation-sensitive green fluorescent protein) in *Arabidopsis*. Plant Physiol. 141, 397–403.
Kangatharalingam, N., Ferguson, M.W., 1984. A simple and rapid technique for fluorescence staining of fungal nuclei. Curr. Microbiol. 10, 99–103.
Klimpel, A., Gronover, C.S., Williamson, B., Stewart, J.A., Tudzynski, B., 2002. The adenylate cyclase (BAC) in *Botrytis cinerea* is required for full pathogenicity. Mol. Plant Pathol. 3 (6), 439–450.
Koc, A., Mathews, C.K., Wheeler, L.J., Gross, M.K., Merrill, G.F., 2006. Thioredoxin is required for deoxyribonucleotide pool maintenance during S phase. J. Biol. Chem. 281, 15058–15063.
Koehler, C.M., Tienson, H.L., 2009. Redox regulation of protein folding in the mitochondrial intermembrane space. Biochim. Biophys. Acta 1793, 139–145.
Kojer, K., Bien, M., Gangel, H., Morgan, B., Dick, T.P., Riemer, J., 2012. Glutathione redox potential in the mitochondrial intermembrane space is linked to the cytosol and impacts the Mia40 redox state. EMBO J. 31, 3169–3182.
Krysan, D.J., 2009. The cell wall and endoplasmic reticulum stress responses are coordinately regulated in *Saccharomyces cerevisiae*. Commun. Integr. Biol. 2, 233–235.
Lacaze, I., Lalucque, H., Siegmund, U., Silar, P., Brun, S., 2015. Identification of NoxD/Pro41 as the homologue of the p22phox NADPH oxidase subunit in fungi. Mol. Microbiol. 95, 1006–1024.
Laloi, C., Rayapuram, N., Chartier, Y., Grienenberger, J.M., Bonnard, G., Meyer, Y., 2001. Identification and characterization of a mitochondrial thioredoxin system in plants. Proc. Natl. Acad. Sci. USA 98, 14144–14149.

Lambeth, J.D., 2004. NOX enzymes and the biology of reactive oxygen. Nat. Rev. Immunol. 4, 181–189.
Lara-Ortiz, T., Riveros-Rosas, H., Aguirre, J., 2003. Reactive oxygen species generated by microbial NADPH oxidase NoxA regulate sexual development in *Aspergillus nidulans*. Mol. Microbiol. 50, 1241–1255.
Levine, A., Tenhaken, R., Dixon, R., Lamb, C., 1994. H_2O_2 from the oxidative burst orchestrates the plant hypersensitive disease resistance response. Cell 79, 583–593.
Lu, J., Holmgren, A., 2014. The thioredoxin antioxidant system. Free Radic. Biol. Med. 66, 75–87.
Malagnac, F., Klapholz, B., Silar, P., 2007. PaTrx1 and PaTrx3, two cytosolic thioredoxins of the filamentous ascomycete *Podospora anserina* involved in sexual development and cell degeneration. Eukaryot. Cell 6, 2323–2331.
Malagnac, F., Lalucque, H., Lepere, G., Silar, P., 2004. Two NADPH oxidase isoforms are required for sexual reproduction and ascospore germination in the filamentous fungus *Podospora anserina*. Fungal Genet. Biol. 41, 982–997.
Marschall, R., Tudzynski, P., 2014. A new and reliable method for live imaging and quantification of reactive oxygen species in *Botrytis cinerea*: technological advancement. Fungal Genet. Biol. 71, 68–75.
Mentges, M., Bormann, J., 2015. Real-time imaging of hydrogen peroxide dynamics in vegetative and pathogenic hyphae of *Fusarium graminearum*. Sci. Rep. 5, 14980.
Mesecke, N., Terziyska, N., Kozany, C., Baumann, F., Neupert, W., Hell, K., Herrmann, J.M., 2005. A disulfide relay system in the intermembrane space of mitochondria that mediates protein import. Cell 121, 1059–1069.
Meyer, A.J., Brach, T., Marty, L., Kreye, S., Rouhier, N., Jacquot, J.P., Hell, R., 2007. Redox-sensitive GFP in *Arabidopsis thaliana* is a quantitative biosensor for the redox potential of the cellular glutathione redox buffer. Plant J. 52, 973–986.
Meyer, Y., Buchanan, B.B., Vignols, F., Reichheld, J.P., 2009. Thioredoxins and glutaredoxins: unifying elements in redox biology. Annu. Rev. Genet. 43, 335–367.
Morgan, B., Sobotta, M.C., Dick, T.P., 2011. Measuring $E_{(GSH)}$ and H_2O_2 with roGFP2-based redox probes. Free Radic. Biol. Med. 51, 1943–1951.
Orrenius, S., Zhivotovsky, B., Nicotera, P., 2003. Regulation of cell death: the calcium-apoptosis link. Nat. Rev. Mol. Cell Biol. 4, 552–565.
Østergaard, H., Henriksen, A., Hansen, F.G., Winther, J.R., 2001. Shedding light on disulfide bond formation: engineering a redox switch in green fluorescent protein. EMBO J. 20, 5853–5862.
Petersen, T.N., Brunak, S., von Heijne, G., Nielsen, H., 2011. SignalP 4.0: discriminating signal peptides from transmembrane regions. Nat. Methods 8, 785–786.
Pontecorvo, G., Roper, J.A., Hemmons, L.M., MacDonald, K.D., Bufton, A.W., 1953. The genetics of *Aspergillus nidulans*. Adv. Genet. 5, 141–238.
Roca, M.G., Weichert, M., Siegmund, U., Tudzynski, P., Fleissner, A., 2012. Germling fusion via conidial anastomosis tubes in the grey mould *Botrytis cinerea* requires NADPH oxidase activity. Fungal Biol. 116, 379–387.
Santos, C.X., Stolf, B.S., Takemoto, P.V., Amanso, A.M., Lopes, L.R., Souza, E.B., Goto, H., Laurindo, F.R., 2009. Protein disulfide isomerase (PDI) associates with NADPH oxidase and is required for phagocytosis of *Leishmania chagasi* promastigotes by macrophages. J. Leukoc. Biol. 86, 989–998.
Sarewicz, M., Osyczka, A., 2015. Electronic connection between the quinone and cytochrome C redox pools and its role in regulation of mitochondrial electron transport and redox signaling. Physiol. Rev. 95, 219–243.
Schumacher, J., de Larrinoa, I.F., Tudzynski, B., 2008. Calcineurin-responsive zinc finger transcription factor CRZ1 of *Botrytis cinerea* is required for growth, development, and full virulence on bean plants. Eukaryot. Cell 7, 584–601.
Schumacher, J., 2012. Tools for *Botrytis cinerea*: new expression vectors make the gray mold fungus more accessible to cell biology approaches. Fungal Genet. Biol. 6, 483–497.
Schumacher, J., Simon, A., Cohrs, K.C., Viaud, M., Tudzynski, P., 2014. The transcription factor BcLTF1 regulates virulence and light responses in the necrotrophic plant pathogen *Botrytis cinerea*. PLoS Genet. 10, e1004040.
Schwarzländer, M., Fricker, M.D., Muller, C., Marty, L., Brach, T., Novak, J., Sweetlove, L.J., Hell, R., Meyer, A.J., 2008. Confocal imaging of glutathione redox potential in living plant cells. J. Microsc. 231, 299–316.
Schwarzländer, M., Fricker, M.D., Sweetlove, L.J., 2009. Monitoring the in vivo redox state of plant mitochondria: effect of respiratory inhibitors, abiotic stress and assessment of recovery from oxidative challenge. Biochim. Biophys. Acta 1787, 468–475.
Scott, B., Eaton, C.J., 2008. Role of reactive oxygen species in fungal cellular differentiations. Curr. Opin. Microbiol. 11, 488–493.
Segmueller, N., Kokkelink, L., Giesbert, S., Odinius, D., van Kan, J., Tudzynski, P., 2008. NADPH oxidases are involved in differentiation and pathogenicity in *Botrytis cinerea*. Mol. Plant Microbe Interact. 21, 808–819.
Semighini, C.P., Harris, S.D., 2008. Regulation of apical dominance in *Aspergillus nidulans* hyphae by reactive oxygen species. Genetics 179, 1919–1932.
Siegmund, U., Heller, J., van Kan, J.A., Tudzynski, P., 2013. The NADPH oxidase complexes in *Botrytis cinerea*: evidence for a close association with the ER and the tetraspanin Pls1. PLoS ONE 8, e55879.
Siegmund, U., Marschall, R., Tudzynski, P., 2015. BcNoxD, a putative ER protein, is a new component of the NADPH oxidase complex in *Botrytis cinerea*. Mol. Microbiol. 95, 988–1005.
ten Have, A., Mulder, W., Visser, J., van Kan, J.A., 1998. The endopolygalacturonase gene Bcpg1 is required for full virulence of *Botrytis cinerea*. Mol. Plant Microbe Interact. 11, 1009–1016.
Thewes, S., 2014. Calcineurin-Crz1 signaling in lower eukaryotes. Eukaryot. Cell 13, 694–705.
Trotter, E.W., Grant, C.M., 2002. Thioredoxins are required for protection against a reductive stress in the yeast *Saccharomyces cerevisiae*. Mol. Microbiol. 46, 869–878.
Tu, B.P., Ho-Schleyer, S.C., Travers, K.J., Weissman, J.S., 2000. Biochemical basis of oxidative protein folding in the endoplasmic reticulum. Science 290, 1571–1574.
Tudzynski, P., Heller, J., Siegmund, U., 2012. Reactive oxygen species generation in fungal development and pathogenesis. Curr. Opin. Microbiol. 15 (6), 653–659.
Viefhues, A., Heller, J., Temme, N., Tudzynski, P., 2014. Redox systems in *Botrytis cinerea*: impact on development and virulence. Mol. Plant Microbe Interact. 27, 858–874.
Yu, S., Qin, W., Zhuang, G., Zhang, X., Chen, G., Liu, W., 2009. Monitoring oxidative stress and DNA damage induced by heavy metals in yeast expressing a redox-sensitive green fluorescent protein. Curr. Microbiol. 58, 504–510.